Composites Part B 258 (2023) 110707

Contents lists available at ScienceDirect

Composites Part B

journal homepage: www.elsevier.com/locate/composites

Effective X-ray micro computed tomography imaging of carbon fibre composites

E.A. Zwanenburg *, D.G. Norman, C. Qian, K.N. Kendall, M.A. Williams, J.M. Warnett

WMG, University of Warwick, CV4 7AL, Coventry, United Kingdom

ARTICLE INFO

Keywords:
CFRP
CF-SMC
X-ray computed tomography
High aspect ratio

ABSTRACT

Compression moulding of carbon fibre sheet moulding compounds is an attractive manufacturing method for composite structures. Investigating fibre orientation, defects and voids in these components is important for quality control. X-ray computed tomography is a non-destructive imaging method used on different kind of sheet moulded compound to identify such issues, but it is still a challenge on carbon fibre sheet moulding compound due to the similarities in density of the carbon fibres and polymer matrix. This study aims to determine the best-practice for optimising acquisition parameters for imaging carbon fibre composites. The first experiment assessed the effect of excess material on a region of interest scans was investigated, a common acquisition approach to maintain resolution to resolve fibres. This showed in this specific case the scan quality decreases when surrounding material reaches approximately 75% of the field of view indicating region of interest scanning is feasible. In the second experiment seven X-ray computed tomography parameters were systematically evaluated to optimise image quality for observing the structures and defects, resulting in 168 scans. The results indicate that the source–detector distance and the source voltage have the most significant impact, where users should always consider maximising this distance and minimising voltage for the best image quality.

1. Introduction

Compression moulding of carbon fibre sheet moulding compound is an attractive option to manufacture high-performance composite parts at a high rate and have a lot of potential in applications such as in the automotive industry due to its low density and ability to be manufactured in complex geometries [1–3]. In the manufacturing process compression makes the fibres and resin flow to the cavities and one of the challenges is the distribution and orientation of the fibres as there could be local variations within the part. As fibre distribution and orientation can have significant impact on the mechanical properties of the component [4], it is important to be able to non-destructively inspect the carbon fibre sheet moulded compound components to visualise the microstructure to improve the quality of the parts and predict their structural behaviour. X-ray computed tomography has been shown to be very suitable to image the fibre orientations in high contrast sheet moulded compound such as glass fibre sheet moulded compounds [5]. The visualisation of carbon fibre sheet moulding compounds is still a challenge in lab-based systems, Fig. 1 shows the variety in lab-based imaging of carbon fibre sheet moulding compounds and their different degrees of image quality.

The main challenge in performing X-ray computed tomography scans of CF-SMC is the low contrast between carbon fibres and polymer resin in the greyscale images. The small difference in attenuation coefficient means images will have a low contrast between the carbon fibres and the resin, making it harder to distinguish them and perform a fibre orientation analysis, and a low voltage is most likely required for contrast [12]. Another issue is the physical size of real industry parts, making it a trade-off between resolution and the scanned volume. A high resolution is required to be able to resolve the individual fibres from the polymer matrix as they are typically 5–7 μm in diameter, but a low voxel size also limits the field of view to small volumes [5]. However, in order to perform a fibre orientation analysis, it is not necessary to be able to observe single fibres, it is sufficient to be able to resolve strands and bundles [13]. It is possible to combine multiple scans to get a 3D volume of full carbon fibre sheet moulding compound parts, but this requires long scanning times [10]. For flat plaques the high aspect ratio also makes scanning more complicated as there is large difference in absorption at different projection angles.

There are examples in literature of X-ray computed tomography scanning of carbon fibre composites, but they follow different scanning approaches and have different objectives or extra challenges in their

* Corresponding author.
E-mail address: Evelien.A.Zwanenburg@warwick.ac.uk (E.A. Zwanenburg).

https://doi.org/10.1016/j.compositesb.2023.110707
Received 19 January 2023; Received in revised form 21 March 2023; Accepted 28 March 2023
Available online 31 March 2023

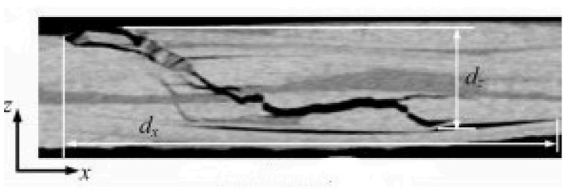

(a) 120 kV, 22.0 μm

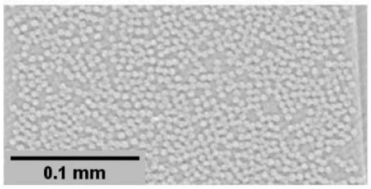

(b) 40 kV, 0.8 μm

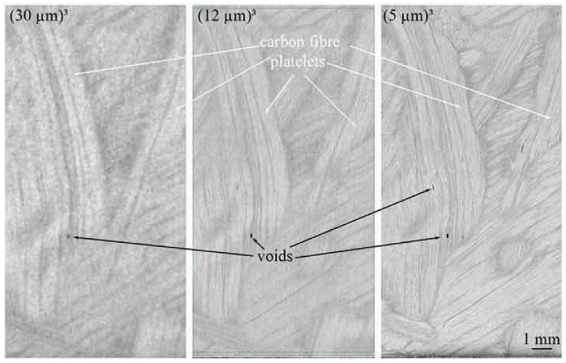

(c) 60 kV, 30μm, 45 kV, 12μm, 60 kV, 5μm

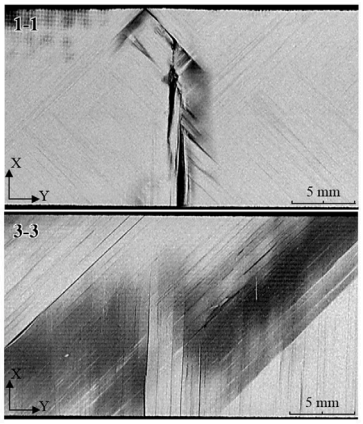

(d) 130 kV, 127 μm

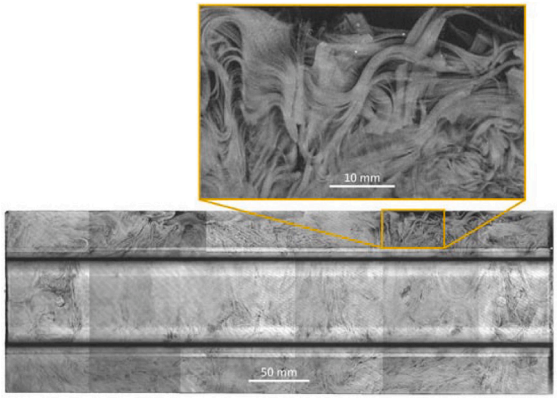

(e) 160 kV, 59.6 μm

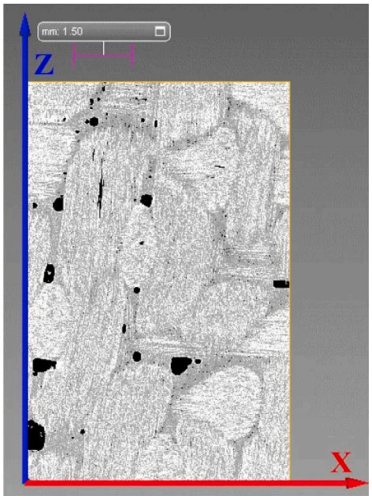

(f) 80 kV, 5 μm

Fig. 1. Examples of carbon fibre sheet moulding compound scanning with their scanning voltage and voxel size, images adapted with permission from (a) [6], (b) [7], (c) [8], (d) [9], (e) [10] and (f) [11].

scanning. For example other materials in the scan require a higher voltage. This is the case for Zhang et al. who required a high voltage of 190 kV due to metal bolt making their data quality not sufficient to distinguish matrix cracks from fibre cracks in their object [14]. Dilonardo et al. scanned their carbon fibre reinforced polymers material at a voltage of 80 kV without a filter and in their analysis the carbon fibre reinforced polymer and pores are separated from each other but not the fibres from the matrix [15]. Another approach is to scan the carbon fibre reinforced polymers samples at a beamline or synchrotron facility where the carbon fibre reinforced polymers can be scanned at a low voltage, but besides accessibility issues most beamlines only allow for a very small sample size making it impractical for scanning larger components, examples can be found in [16,17]. Teuwsen et al. stitched multiple scans together to have a full 3D volume of a larger component (150 mm × 450 mm × 52 mm) (Fig. 1(e)) [10]. They use a relatively high voltage of 160 kV, voxel size of 60 μm and a single scan takes 100 min. A filter was added to reduce the beam hardening effects. While Stelzer et al. use lower voltages (45–60 kV) with voxel sizes ranging from 5 μm to 30 μm with scan times of at least 114 min (Fig. 1(c)) [8]. This shows there is no uniform strategy for scanning carbon fibre sheet moulded compound components and also the scan time is relatively long. Zehnder et al. varied their parameters in their study to track the deformation of fibres in composite laminates during high strain bending (Fig. 1(b)) [7]. They found that longer scans, which in their case meant using a longer source–detector distance (SDD), and a low voltage of 40 kV gave better results than scanning with a shorter source–detector distance at a higher voltage of 100 kV, but their scans were performed with a Zeiss Versa X-ray microscope that can only scan very small samples and they also used phase contrast imaging to reduce noise and increase contrast.

This study optimises the acquisition strategy for carbon fibre composites to maximise image quality for visualising the fibres, observing defects and performing an orientation analysis. It adds to the understanding of how to tweak acquisition parameters to optimise the image

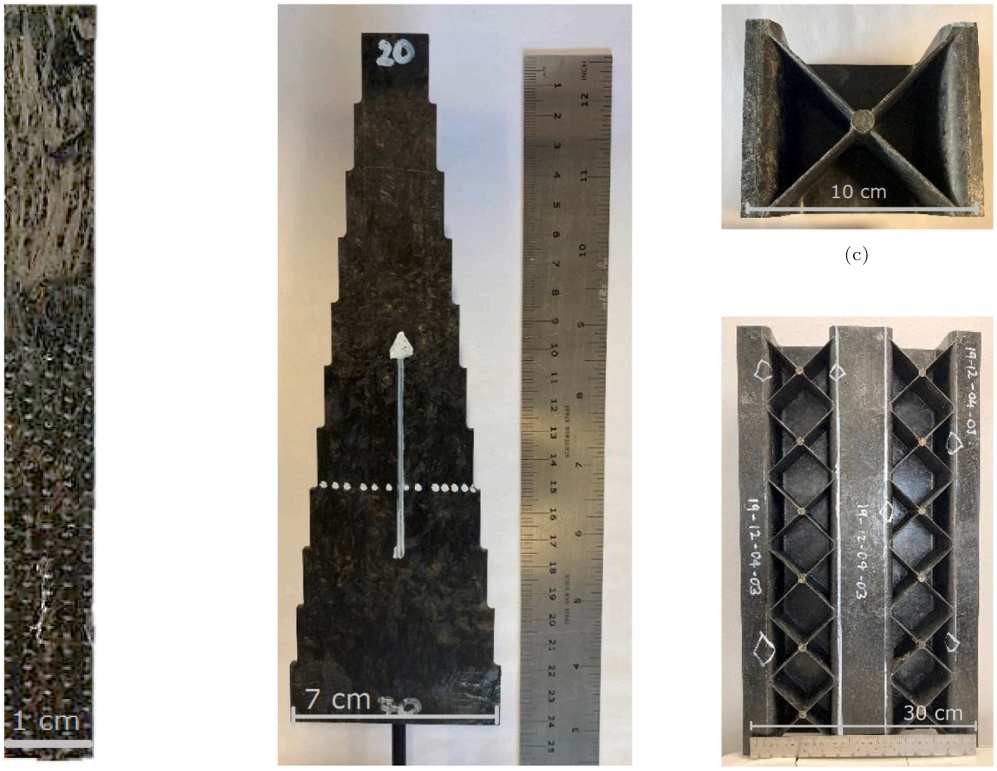

(a) (b) (c) (d)

Fig. 2. The different objects used in this study; (a) single CF piece, (b) flat plaque with increasing width, (c) sample cut from W-profile and (d) W-profile.

quality for a given resolution as different X-ray systems can have a different output for the same parameters depending on their hardware such as the brightness of the source or the detector sensitivity. First, the effect of plate size and surrounding material on region of interest scans of carbon fibre sheet moulded compounds has been studied to explore the option to use X-ray computed tomography on larger parts and increasing aspect ratio as would be the case for manufactured parts (experiment 1). The second experiment systematically tests seven acquisition parameters that have been systematically tested and the images assessed on different aspects with a focus on contrast and resolution (experiment 2).

2. Method

The material used in this study is a structural carbon fibre sheet moulded compound manufactured by Toray Industries Inc. The sheet moulded compound material has a nominal fibre length of 12.5 mm and fibre weight fraction of 57%, and a styrene free vinylester resin system. Due to reasons of confidentiality, further details about the material will not be disclosed in this paper. The carbon fibre sheet moulded compound was moulded in a flat plaque geometry with dimensions of 550 mm × 550 mm × 2 mm with an Engel V-Duo 1700 tonne press. The plaque was cut in samples of different widths to scan with a UniTOM XL (TESCAN, Czech Republic) X-ray computed tomography scanner. Fig. 2 shows the different parts used in this study: from single CF piece to optimise acquisition parameters and a flat plate to investigate the effect of excess material used in the experiments to a realistic manufactured part, the W-profile.

The scans were reconstructed using a filtered back projection algorithm and afterwards the slices were aligned and cross sections for image analysis were selected approximately in the centre of the plate using VGStudio MAX 3.0 (Volume Graphics GmbH, Germany). Further numerical analysis of image quality on this slice in experiment 2 was performed in MATLAB.

Table 1
X-ray computed tomography parameters for experiment 1 performed with an UniTOM XL (TESCAN, Czech Republic).

X-ray computed tomography parameters experiment 1	
Voltage (kV)	40
Power (W)	15
Voxel size (μm)	10
Exposure time (ms)	300
Averages	5
Source-detector distance (mm)	500
Projections	3014
Detector (pixel)	1920
Binning	1
Scanning mode	Smooth
Filter	No filter

3. Experiment 1 — Aspect ratio and region of interest issues

3.1. Experimental setup

This experiment tested the impact of excess material on the image quality of a fixed region of interest scan. In order to test this a sample was cut to cascade with increasing width such that the plaque width increased in steps of 25% percent compared to the top, see Fig. 3. The sample was scanned in nine steps with a fixed region of interest starting from the top. The acquisition parameters for these scans can be found in Table 1, all scans had a field of view of 20 mm × 20 mm and the parameters were optimised for the smallest part of the sample (0% excess material).

3.2. Results

The results of experiment 1 are shown in Fig. 3. As different parts of one sample have been scanned in this experiment instead of the

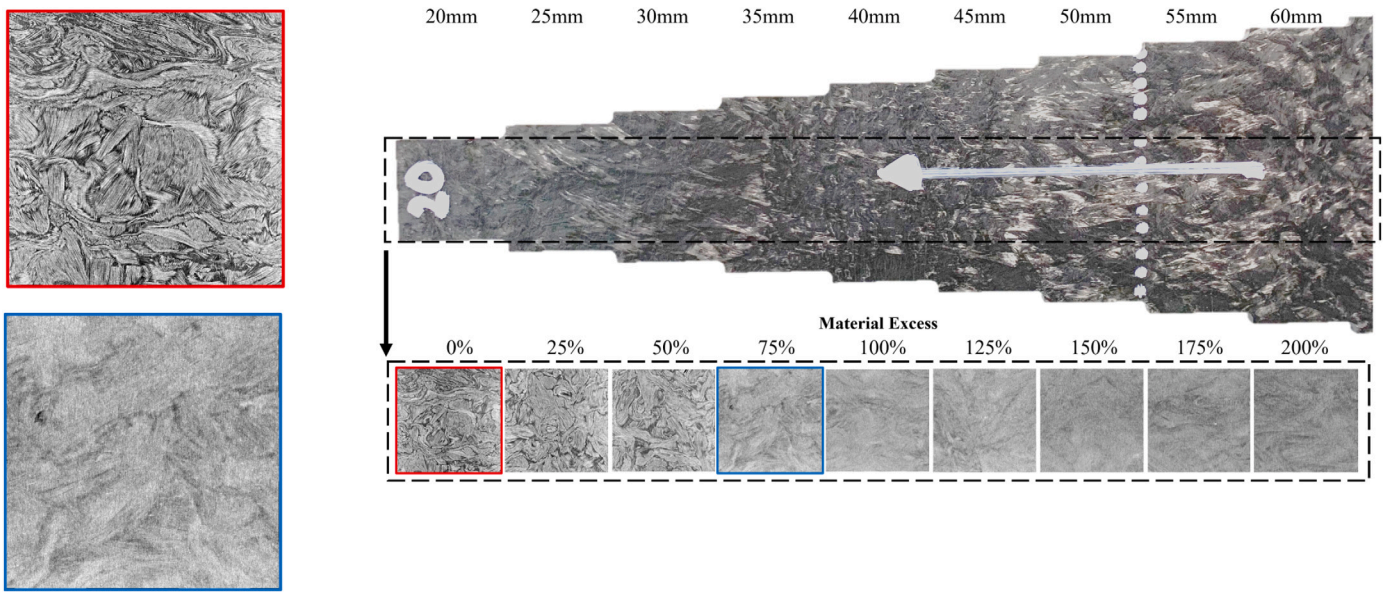

Fig. 3. The results of experiment 1 with the images of the slices obtained with the settings in Table 1. The black dotted line indicates the field of view of the scan and as can be seen the excess material linearly increases from no excess material to 200% excess material. On the left are enlarged images of 0% and 75% excess material.

same sample multiple times, the cross sections are not the same. There is a clear cut-off between the 50% and 75% excess material cross sections in contrast and sharpness, this indicates that in the case of flat plaques up to 50% surrounding material is acceptable for X-ray computed tomography scanning where a greater amount of material excess will result in a clear drop in image quality. This suggests there is a limit to scanning local region of interest in carbon fibre sheet moulded compound samples.

It was not possible to perform an quantitative image quality analysis as the images are not from the same cross section and there was too much variation between slices of each region of interest.

4. Experiment 2 — Acquisition strategies for quality

4.1. Experimental setup

In this experiment seven acquisition parameters were systematically tested to obtain the optimal scanning strategy for carbon fibre sheet moulded compounds with the experimental method depicted in Fig. 4. The sample used in this experiment had a width of 9.6 mm and was positioned in the scanner such that an area of 9.6 mm × 9.6 mm only just filled the field of view for the baseline scan. The sample alignment was not changed during the scans to be able to compare the same cross section for all scans.

Seven different X-ray computed tomography acquisition parameters have been manipulated: sample rotation, number of projections, number of averages, power, voltage, voxel size and source–detector distance. They influence the scanning process on different aspects:

- In most X-ray computed tomography systems there are two different **scanning modes**: stop/start and smooth with the difference whether the stage stops rotating for each projection or keep turning during the projections, which makes smooth scanning faster.
- The **number of projections** that should be taken during a 360° rotation for filtered back projection reconstruction is usually determined using the Nyquist sampling rule:

$$\frac{\pi}{2} * \langle windowsize/\text{pixel} \rangle \quad (1)$$

and is based on the width of the detector. The number of projections was adjusted as a percentage of the Nyquist criterion, where 100% was the baseline.

- The **number of averages** is the number of projections the detector collects at one angle and subsequently averages into one projection, this reduces the noise in the image.
- The source **power** is both related to the photon intensity and the resolution: a higher power will increase the number of photons per time unit, but the spot size of the beam increases with the power, which can cause blurring when it is above the voxel size.
- The source **voltage** sets the maximum energy of the X-ray spectrum, depending on the X-ray absorption coefficients of the scanned this decreases the likelihood of the photons to be absorbed. In general voltage is set to have a value based on the material, a higher (X-ray) density requires a higher voltage.
- The **voxel size** is dependent on the magnification. To be able to resolve features the voxel size is required to be smaller than the feature of interest, in this case the carbon fibres tows.
- The **source–detector distance** can be changed in the used X-ray computed tomography system, but this is not possible in all X-ray computed tomography systems. A shorter source–detector distance will give a brighter image as it follows the inverse square law for intensity. A long source–detector distance therefore means a longer acquisition time, but with a higher contrast.

More detail on individual acquisition parameters and their impacts on image quality and speed can be found in [12].

When a selected parameter was changed the exposure time was adjusted such that the maximum grey value count would be 51k to maximise the use of the dynamic range. Since some parameter settings were sub optimal in contrast the minimum in the grey value dynamic range varied significantly from 20–28k. In the used system changing the detector gain is not part of the normative process, in other systems this may be possible and it can be a suitable option to increase the brightness without increasing the acquisition time. This resulted in 56 scans with different settings changed from the baseline scan, see Table 2 for the baseline acquisition parameters. The baseline scan had an acquisition time of 7 min, the shortest scan took 2.1 min (1 average) and the longest 2 h and 25 min. This set of scans had a total scan time of 16 h and was repeated three times. The acquisition parameters of the initial scan were decided by test scans and scan time considerations, such as a small field of view.

Images of the different voxel sizes are included, but 10 μm was chosen throughout to be able to observe the necessary feature. Increasing

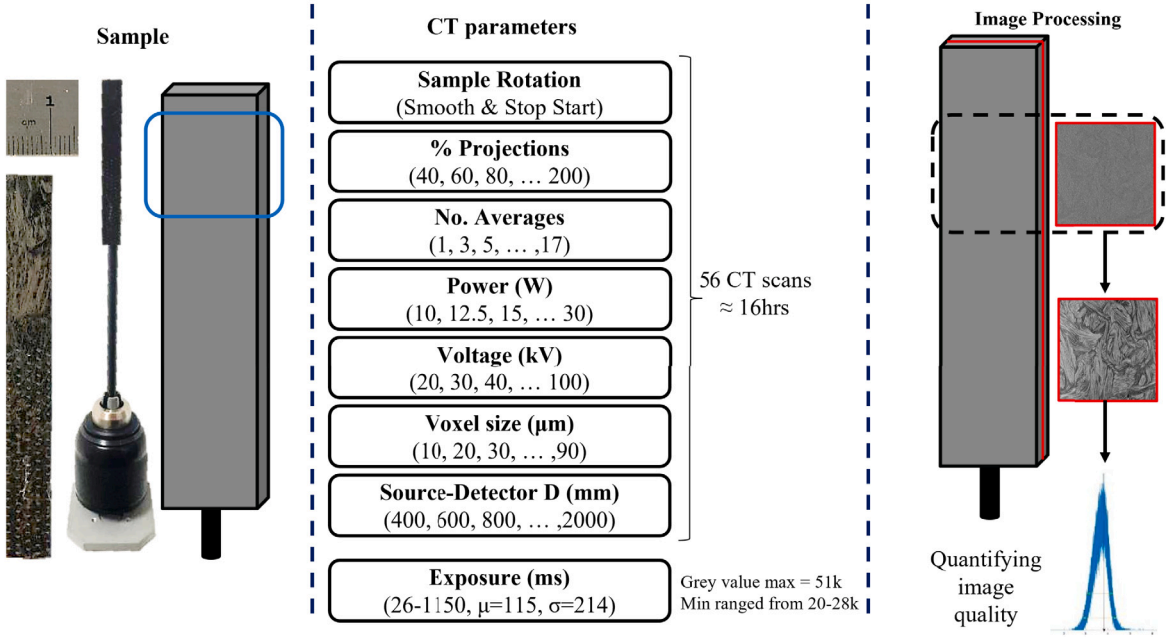

Fig. 4. The method of experiment 1, from left to right: the sample, the tested parameters with the tested values and the image processing from reconstruction to alignment and histograms.

Table 2
Baseline acquisition parameters experiment 2 performed with an UniTOM XL (TESCAN, Czech Republic).

XCT baseline parameters experiment 2	
Voltage (kV)	40
Power (W)	15
Voxel size (µm)	10
Averages	5
Source-detector distance (mm)	400
Projections	1507
Detector (pixel)	1920
Binning	2
Scanning mode	Smooth

Table 3
The optimal parameters for best image quality from the qualitative assessment in experiment 2.

The optimal parameters	
Voxel size (µm)	10
Power (W)	20
Voltage (kV)	40
Number of averages	5
Source-detector distance (mm)	2000
Projections (percentage Nyquist)	100%

the voxel size would make it hard to distinguish the tows as they would be represented by a lower number of voxels, which increases partial volume effects.

4.2. Visual assessment

The cross section of experiment 2 are shown in Fig. 5, it is the same slice for every set of acquisition parameters in order to compare them and the inset shows the acquisition time. The images show differences in contrast, noise and sharpness and it is clear that some parameters have a greater effect on the image quality than others. The following observations can be made when comparing the rows individually:

- The expectation when changing the number of **averages** the noise decreases, which indeed is observed in the images, but after 5 averages there is no clear visual improvement.
- A number of projections significantly lower than the Nyquist criterion introduces more noise and artefacts in the images. Increasing the number of projections does not improve the image quality visually.
- The source–detector distance shows to have a big impact on the contrast which improves for every step, but increasing the source–detector distance increases the acquisition scan time significantly. A scan at a source–detector distance of 2000 mm takes 16 times as long as a scan at 500 mm.
- The scans with a source power below 20 W look similar in terms of sharpness, when the power increases the images get more blurred. By eye, fibre bundles cannot be observed any more at a power of 30 W. This behaviour corresponds to the focal spot size of the used X-ray computed tomography system that increases with the power.
- The voltage has both an effect on the contrast and the noise. The lower voltages give a better contrast, but very low voltages tend to be less stable in most lab-based X-ray computed tomography systems. This is also the case in the used machine as can be observed in the image of 20 kV.
- There is no visible difference between the smooth or stop–start scan mode. So there is in this case no benefit to choose the stop–start mode as this increases the scan time.

The assessment indicates that a low voltage and large source–detector distance have the most impact on the contrast between the carbon fibres and the resin, the optimal parameters are summarised in Table 3. There is no observable benefit in increasing the number of projections over the Nyquist sampling rule, setting the number of averages above 5 or using stop–start scan mode. For the choice of the power the focal spot size is important in combination with the chosen voxel size.

4.3. Quantitative assessment

Fig. 6 shows a cross section of the baseline scan with its grey value histogram. In the presented slice one can observe two materials; the resin and the carbon fibre. There is no observable air around

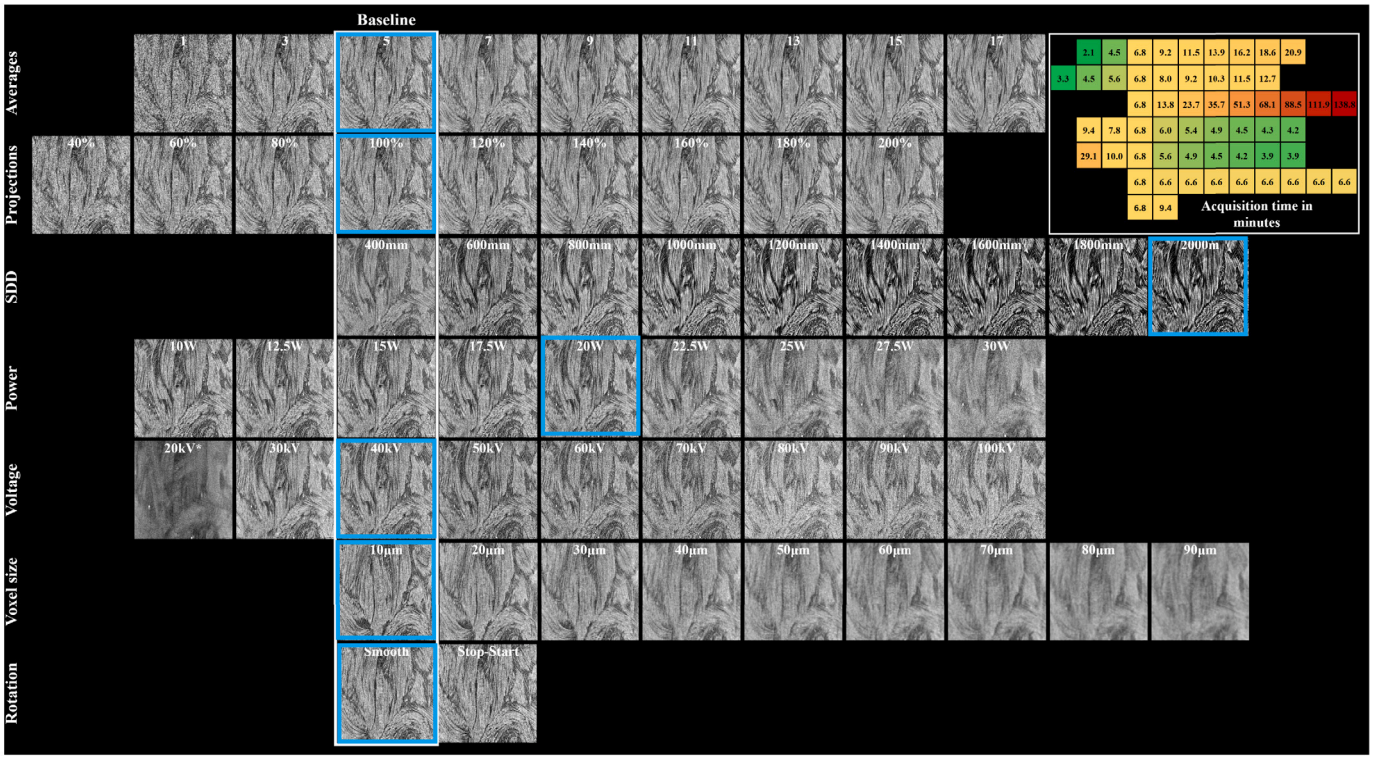

Fig. 5. An overview of the results of experiment 2, it shows cross sections of the same area for each scan. Every row is one manipulated parameter and the cross sections in the white box all have the same baseline settings, see Table 2, the blue boxes to the optimal parameters from qualitative assessment in Table 3. The inset shows the acquisition times in minutes. (For interpretation of the references to colour in this figure legend, the reader is referred to the web version of this article.)

the part or porosity so one would not observe this in the histogram as a third material peak. However, because of the relatively similar densities of the two materials, instead of showing a bi-modal which would make it easy to separate the two, it is a single peak. This is the case for all images of these experiments and caused by the similar attenuation coefficients of the carbon fibres and resin. Therefore, it is not possible to use the normative image quality metrics that are based on a histogram with two (or more peaks) such as the signal-to-noise ratio or contrast-to-noise ratio which use the mean of the peaks (signal) and their standard deviation (noise) as a measure of image quality. A parameter that can be used is the anisotropy, this is a measure of the directional entropy that correlates with noise and sharpness of the image [18]. It is based on the Rényi Entropy Measures, which is derived from the Shannon entropy, and the one-dimensional Pseudo-Wigner Distribution. It is a measure for image quality without a reference, aimed at selecting the best image of a set of images

It is defined as:

$$R_\alpha = \frac{1}{1-\alpha}\log_2\left(\sum_n \sum_k P^\alpha[n,k]\right) \tag{2}$$

where n and k are respectively the spatial and frequency variables. It measures the averaged anisotropy using a pixel wise directional entropy. As can be seen in the case of α approaching 1 this becomes the Shannon Entropy, more information can be found in [18]. The anisotropy was calculated using a Matlab script by Gabarda with as input variables a window size of 8 pixels, 6 directions and 0 degrees as the first angle [19]. The results are shown in Fig. 7.

The visual assessment implied there was little to be gained in increasing the number of averages above 5, and projections beyond 100% but the anisotropy implies it does, this could indicate an improvement not visible for the eye. For the source–detector distance there is a far more notable increase in anisotropy, 20 times more than averages or projections, but having shorter source–detector distance than the baseline did not decrease as much as expected.

Considering the three different aspects of image quality contrast is the most challenging to achieve when scanning carbon fibre sheet moulded compounds. An appropriate spot size should provide sharpness and noise can be reduced by maximising the dynamic range and a sufficient photon count. As the histogram of both the signal and background signal are one peak an interesting number to investigate would be the standard deviation of a Gaussian curve fitted to this peak. This could be seen as a measure of the width of the signal peak. Unfortunately this width is affected by both the noise and the contrast, in fact they give competing effects that increase and decrease the width. When considering two materials of very similar grey values:

- A higher contrast means separation of the materials, a larger standard deviation and therefore a broader peak.
- A lower amount of noise means a smaller standard deviation and therefore a narrower peak.

It is thus important to consider on which aspect of image quality an acquisition parameter will affect in order to be able to assess if it improves or worsens.

Gaussian curves were fitted to the single peak grey value histograms using Matlab. The standard deviation of the three repeats were averaged and the results can be found in Fig. 8. In order to compare the impact of each parameter it shows the values normalised against the baseline values. Looking at each individual parameter the following can be observed:

- The voltage impacts the contrast, a higher voltage means lower contrast and therefore a smaller standard deviation. In the graph the instability of the X-ray source at very low kV, in this case 20 kV, is reflected by the large error bar and the (stable) lower values have a wider histogram compared to the higher voltages, but not to the extent that was expected in the qualitative assessment due to the decrease in contrast.

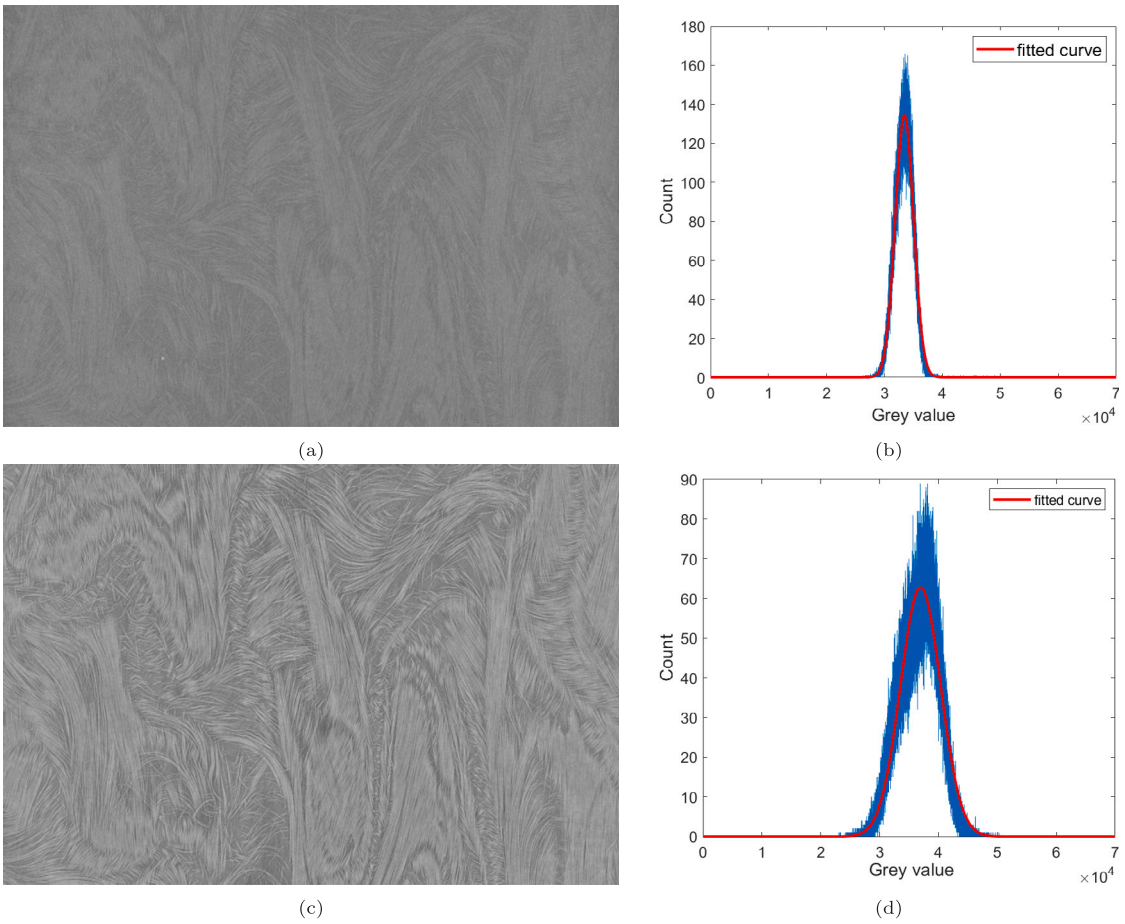

Fig. 6. (a) Reconstructed and aligned cross section of experiment 1 with baseline settings. (b) Grey value histogram of (a). (c) Reconstructed and aligned cross section of experiment 1 with a source–detector distance of 2000 mm. (d) Grey value histogram of (c).

- The power impacts the sharpness at the edges, a higher power results in a lower sharpness and therefore more intermediate grey scale values and less of the extreme values, which would translate to a narrower standard deviation. This is also observed in the graph. The power shows the expected behaviour as the standard deviation drops down when it is larger than the voxel size
- The number of averages impacts the noise and less noise will results in a smaller standard deviation. As seen before, the first steps of increasing the number of averages has significant impact, while increasing beyond 5 averages has barely any impact.
- The source–detector distance has impact on all three aspects of image quality. The source–detector distance shows an improvement with approximately linear steps of width increase as would be expected as the noise decreases when the source–detector distance increases. This behaviour was, for lower values, not visible in the anisotropy graph.
- The number of projections, the noise is the dominating factor, thus less noise and a smaller standard deviation are preferred. The figure with the number of projections confirms that also in this case increasing beyond the Nyquist criterion has no benefit. A number of projections below the criterion decreases the width of the peak, but the resulting images are worse than the numbers indicate most likely due to the increase of noise balancing the loss in sharpness in the width of the histogram peak.

When comparing the impact of each parameter by normalising the standard deviation graphs on the baseline parameter values, it is directly observable that the source–detector distance has the most impact on the width of the peak, as it approximately increases from 1 at 400 mm to 3 at 2000 mm. The number of averages has a range of approximately 0.5 and the other parameters have an even lower impact. It is worth noting that the number of averages and the source–detector distance have the most impact on the acquisition time indicating that for carbon fibre reinforced polymers very long scans will give the best contrast.

5. Application

To show how the results of experiment 1 and 2 can be used to scan and inspect more complicated samples than flat plate samples, a W-profile was scanned using three different acquisition strategies with the results shown in Fig. 9. The W-profile had a sheet thickness of 3 mm, dimensions of 600 mm × 340 mm × 60 mm and rib sections with a width of 80 mm. The circular intersection point of the ribs has a diameter of 10 mm. First a full scan of the object was performed. Because the object is relatively large, the scan had a lower voxel size (120 μm) and a higher voltage was required to have sufficient penetration of the X-rays, this also introduced the requirement for a filter to reduce beam hardening. The second approach was a region of interest scan, such that only that part of the object was in the field-of-view. In this case still a higher voltage is required, but the voxel size reduced to 50 μm. For third scan a sample that fits in the field-of-view was cut from the W-profile, in this case it was possible to lower the voltage as there was less material between the source and detector and the resolution was the same as the region of interest scan.

Commonly either a full object is scanned or a subsample is cut from a larger sample to be able to reach the required resolution. Thus obtaining the required information from the sample without having to cut the

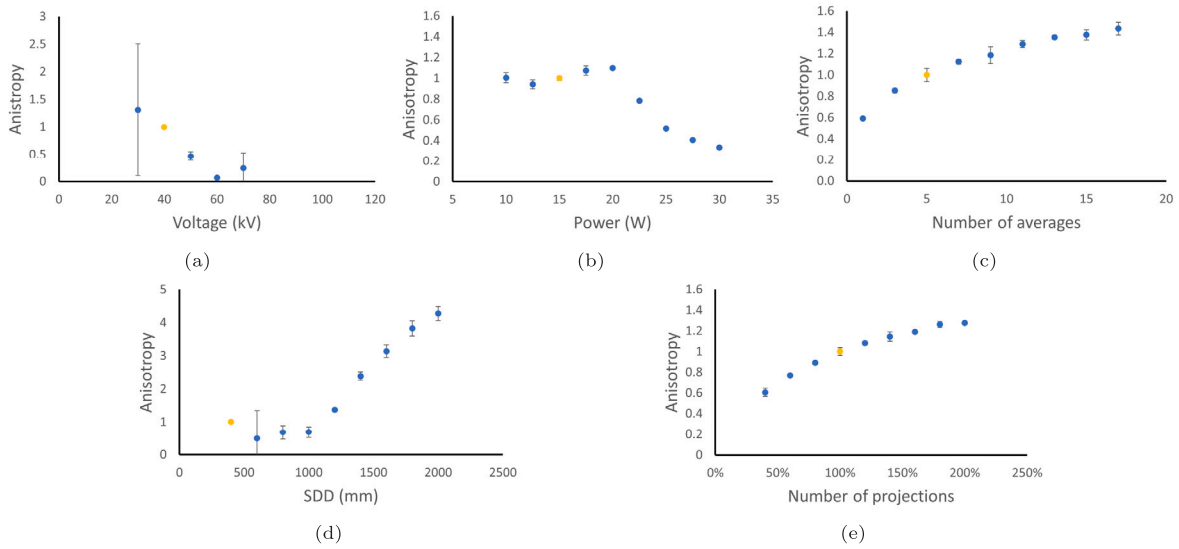

Fig. 7. The anisotropy results (normalised on the baseline value of each series) of (a) voltage, (b) power, (c) number of averages, (d) source–detector distance, (e) number of projections. The baseline is indicated in orange, the vertical axes are not the same and the error bar is the standard deviation between the measurements. (For interpretation of the references to colour in this figure legend, the reader is referred to the web version of this article.)

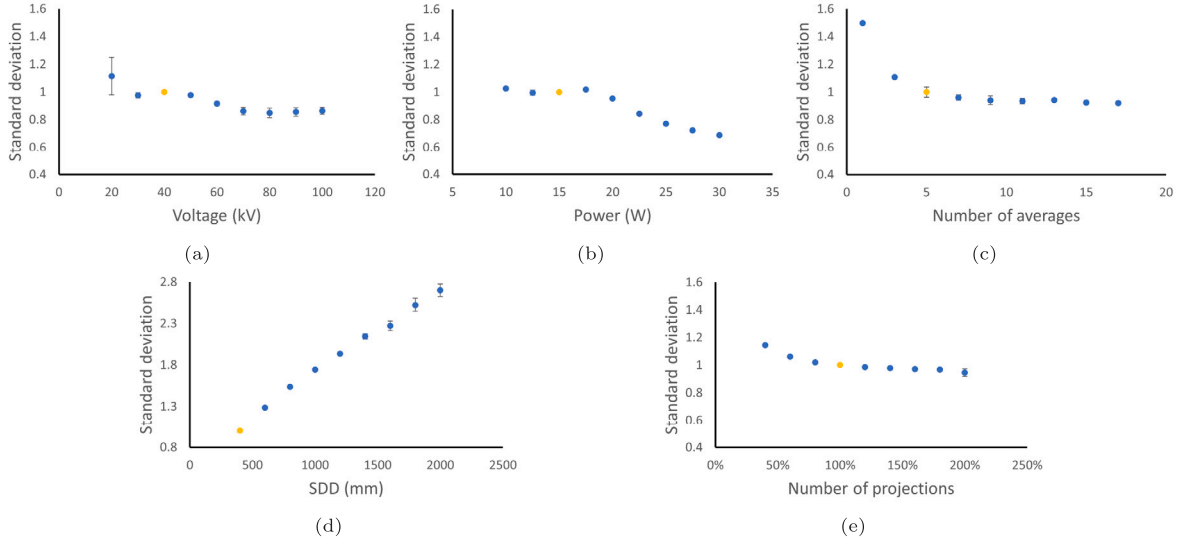

Fig. 8. The standard deviation of the fitted Gaussian (normalised on the baseline value of each series) (a) voltage, (b) power, (c) number of averages, (d) source–detector distance, (e) number of projections. The baseline is indicated in orange, the vertical axes are not the same and the error bar is the standard deviation between the measurements. (For interpretation of the references to colour in this figure legend, the reader is referred to the web version of this article.)

sample is preferable. The enlarged images in Fig. 9 show the region of interest scan gives similar contrast to the scan of the subsample, this shows it is a viable option to use region of interest scanning for carbon fibre sheet moulded compound objects while applying the principles of parameter selection discussed in the previous experiment.

6. Discussion

Scanning a carbon fibre sheet moulded compound component in its entirety at sufficient resolution requires in most cases multiple stacked scans. Often only certain areas are of interest, so-called region of interest scanning would be an alternative that could save a significant amount of scan time. Experiment 1 showed region of interest scans are possible and while quantitative analysis with image quality metrics was not possible as the cross section were not from the same location in the sample. For excess material greater than the diameter of the field of view the limit for excess material could be put between 50% and 70%. In this experiment the choice was made to use a flat plaque object and not a stepped cylinder to study the influence of excess material as carbon fibre products and objects often have a high-aspect ratio. The conclusions could be different in case of a cylindrical object. Also the acquisition parameters were optimised for the top part of the flat plaque object and thus the X-rays will struggle to get through the increased material on the long axis.

Experiment 2 showed the effects of the different acquisition parameters on the image quality but the acquisition time was not taken into account when deciding the best acquisition parameters. Furthermore increasing the acquisition time of a short 'bad' scan could result in a similar or even better image compared to a very good scan with a very long acquisition time. For example scanning at a short(er) source–detector distance with a higher number of averages could improve the images while still having a similar or shorter acquisition time compared to a long source–detector distance. It depends on the application whether image quality or scan time is of greater importance.

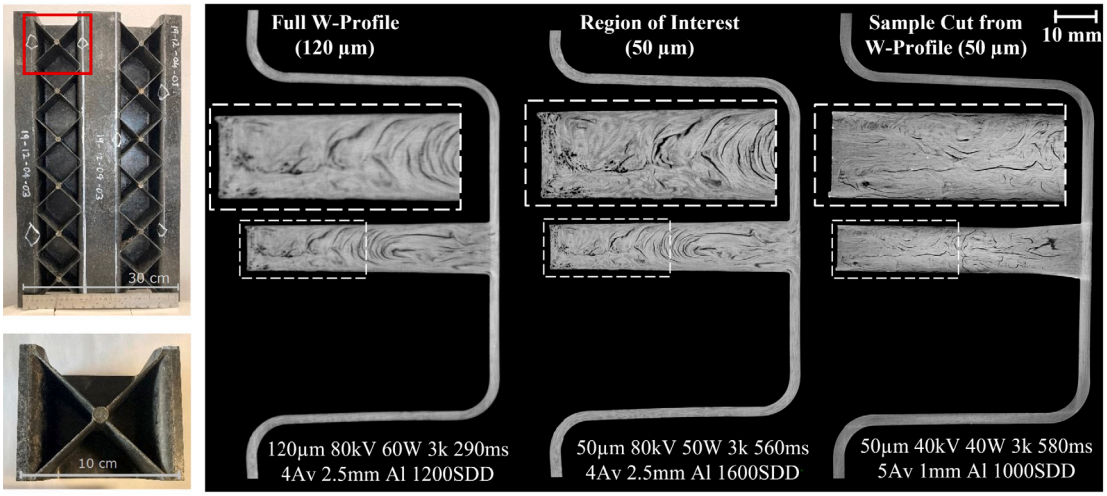

Fig. 9. A W-profile scanned with three different approaches: left full scan, middle a region of interest scan and right a sample cut from the W-profile (approximately 100 mm × 100 mm). Below each approach are the used acquisition parameters, the red box indicates the scanned area and the white boxes show the area of the enlarged area. (For interpretation of the references to colour in this figure legend, the reader is referred to the web version of this article.)

Quantitative image assessment to determine the best image is a challenge and thus determining the best acquisition parameters is often completely objective. Using image quality metrics can help to quantify the best scan but still requires caution as metrics do not assess the full image quality, only aspects of it. In this case standard grey level histogram image quality metrics were not an option, but the width of the single peak in the histogram was used as an alternative to measure the contrast. This resulted some indications of the contrast improvement, but this method is also sensitive to noise.

With more realistic test samples such as the W-profile shown, focusing on regions of interest to increase the resolution is key. The principals of minimising the voltage to maximise contrast were similarly applied, although slightly higher and the introduction of a filter was required due to the volume of material penetrated compared to the initial study. This has helped to enhance the visibility of the pores within the rib section and while individual fibres are not clear due to the resolution, fibre bundles and resin rich regions can be well distinguished.

7. Conclusion

The first experiment region of interest scanning is limited by the size of the sample as in this case with 75% or greater excess material the image quality drops significantly indicating region of interest scanning can be a feasible option for scanning carbon fibre composites. The second experiment systematically tested a range of X-ray computed tomography acquisition parameters and showed it is possible to scan carbon fibre sheet moulded compound and obtain sufficient contrast to resolve fibre bundles. In particular it highlighted that voltage and the source–detector distance have the most significant impact on the image contrast, as shown both in visual observations and quantitative evaluation using the standard deviation of the grey value histogram peak as a measure of contrast and anisotropy as an indicator of noise. Although not every X-ray system offers the same flexibility in setting the acquisition parameters the results add to the understanding of how to adjust them for carbon fibre composites. A low voltage is preferable for scanning carbon fibre sheet moulded compounds, but this is limited to maintaining sufficient penetration through the sample as was observed in the subsequent experiment; the shape and composition of the sample can limit the freedom of setting the parameters as a certain voltage is required for penetration. A long source–detector distance resulted in a very good contrast, but the costs in terms of scanning time are very high and not all X-ray computed tomography systems have a variable source–detector distance.

Using the findings of experiments a 360 mm diameter W-profile was scanned first at low resolution containing the whole part, and secondly focusing on a region of 150 mm diameter region of interest around a rib. Given the much larger size of the part versus the previous more fundamental experiment, a voltage of 80 kV was the smallest possible to maintain the resolution but also to achieve sufficient penetration. The region of interest scan was compared to that of the region physically cut out of the W profile and scanned in its of right. The three different scans showed that region of interest scanning is a suitable method for carbon fibre sheet moulded compound objects. Overall, X-ray computed tomography imaging was shown to be a powerful non-destructive tool for visualising tows of fibres and defects in carbon fibre sheet moulded compounds with this study highlighting key processes and parameters to enable the highest quality scans in the lab.

CRediT authorship contribution statement

E.A. Zwanenburg: Investigation, Data curation, Formal analysis, Visualization, Writing – original draft. **D.G. Norman:** Conceptualization, Methodology, Investigation, Formal analysis, Visualization. **C. Qian:** Conceptualization, Resources, Funding acquisition. **K.N. Kendall:** Resources, Funding acquisition, Supervision. **M.A. Williams:** Resources, Supervision. **J.M. Warnett:** Conceptualization, Methodology, Writing – review & editing, Supervision.

Declaration of competing interest

The authors declare that they have no known competing financial interests or personal relationships that could have appeared to influence the work reported in this paper.

Data availability

Data will be made available on request.

Acknowledgements

This work was supported by the EPSRC Future Composites Manufacturing Hub, United Kingdom (EP/P006701/1), the EPSRC Future Metrology Hub, United Kingdom (EP/P006930/1), the EPSRC Strategic Equipment Award, United Kingdom (EP/S010076/1) and the National Research Facility in X-ray Computed Tomography, United Kingdom Grant (EP/T02593X/1). We would like to acknowledge Toray Automotive Centre Europe (AMCEU) for donating the material used in this study.

References

[1] Yao SS, Jin F-L, Rhee KY, Hui D, Park S-J. Recent advances in carbon-fiber-reinforced thermoplastic composites: A review. Composites B 2018;142:241–50. http://dx.doi.org/10.1016/j.compositesb.2017.12.007.

[2] Wakekar AD, Patil SH, Deshmukh S, Thakar CM. The review of carbon fiber materials in automotive industry. ECS Trans 2022;107(1):16595. http://dx.doi.org/10.1149/10701.16595ecst.

[3] Ahmad H, Markina AA, Porotnikov MV, Ahmad F. A review of carbon fiber materials in automotive industry. IOP Conf Ser: Mater Sci Eng 2020;971(3):032011. http://dx.doi.org/10.1088/1757-899X/971/3/032011.

[4] Kuhn C, Walter I, Taeger O, Osswald TA. Experimental and numerical analysis of fiber matrix separation during compression molding of long fiber reinforced thermoplastics. J Compos Sci 2017;1(1):2. http://dx.doi.org/10.3390/jcs1010002.

[5] Garcea SC, Wang Y, Withers PJ. X-ray computed tomography of polymer composites. Compos Sci Technol 2018;156:305–19. http://dx.doi.org/10.1016/j.compscitech.2017.10.023.

[6] He Y, Mei M, Wei K, Yang X, Duan S, Han X. Interlaminar shear behaviour and meso damage suppression mechanism of stitched composite under short beam shear using X-ray CT. Compos Sci Technol 2022;218:109189. http://dx.doi.org/10.1016/j.compscitech.2021.109189.

[7] Zehnder AT, Patel V, Rose TJ. Micro-CT imaging of fibers in composite laminates under high strain bending. Exp Tech 2020;44(5):531–40. http://dx.doi.org/10.1007/s40799-020-00374-9.

[8] Stelzer PS, Plank B, Major Z. Mesostructural simulation of discontinuous prepreg platelet based carbon fibre sheet moulding compounds informed by X-ray computed tomography. Nondestruct Test Eval 2020;35(3):342–58. http://dx.doi.org/10.1080/10589759.2020.1774584.

[9] Djabali A, Toubal L, Zitoune R, Rechak S. Fatigue damage evolution in thick composite laminates: Combination of X-ray tomography, acoustic emission and digital image correlation. Compos Sci Technol 2019;183:107815. http://dx.doi.org/10.1016/j.compscitech.2019.107815.

[10] Teuwsen J, Hohn SK, Osswald TA. Direct fiber simulation of a compression molded ribbed structure made of a sheet molding compound with randomly oriented carbon/epoxy prepreg strands—A comparison of predicted fiber orientations with computed tomography analyses. J Compos Sci 2020;4(4). http://dx.doi.org/10.3390/jcs4040164.

[11] Dilonardo E, Nacucchi M, De Pascalis F, Zarrelli M, Giannini C. Inspection of carbon fibre reinforced polymers: 3D identification and quantification of components by X-ray CT. Appl Compos Mater 2022;29(2):497–513. http://dx.doi.org/10.1007/s10443-021-09976-x.

[12] Zwanenburg EA, Williams MA, Warnett JM. Review of high-speed imaging with lab-based x-ray computed tomography. Meas Sci Technol 2022;33(1):012003. http://dx.doi.org/10.1088/1361-6501/ac354a.

[13] Denos BR, Sommer DE, Favaloro AJ, Pipes RB, Avery WB. Fiber orientation measurement from mesoscale CT scans of prepreg platelet molded composites. Composites A 2018;114:241–9. http://dx.doi.org/10.1016/j.compositesa.2018.08.024.

[14] Zhang H, Li C, Dai W, Liu Y, Tian S, Huang W, Jia D, He D, Zhang Y. Static compression testing CFRP single-lap composited joints using X-ray μCT. Compos Struct 2020;234. http://dx.doi.org/10.1016/j.compstruct.2019.111667.

[15] Dilonardo E, Nacucchi M, De Pascalis F, Zarrelli M, Giannini C. High resolution X-ray computed tomography: A versatile non-destructive tool to characterize CFRP-based aircraft composite elements. Compos Sci Technol 2020;192. http://dx.doi.org/10.1016/j.compscitech.2020.108093.

[16] Sencu RM, Yang Z, Wang YC, Withers PJ, Soutis C. Multiscale image-based modelling of damage and fracture in carbon fibre reinforced polymer composites. Compos Sci Technol 2020;198:108243. http://dx.doi.org/10.1016/j.compscitech.2020.108243.

[17] Pei S, Wang K, Li J, Li Y, Zeng D, Su X, Xiao X, Yang H. Mechanical properties prediction of injection molded short/long carbon fiber reinforced polymer composites using micro X-ray computed tomography. Composites A 2020;130:105732. http://dx.doi.org/10.1016/j.compositesa.2019.105732.

[18] Gabarda S, Cristóbal G. Blind image quality assessment through anisotropy. J Opt Soc Amer A 2007;24(12):B42–51. http://dx.doi.org/10.1364/JOSAA.24.000B42.

[19] Gabarda S. Blind image quality assessment through anisotropy. 2015, https://www.mathworks.com/matlabcentral/fileexchange/30800-blind-image-quality-assessment-through-anisotropy.